Zeitschrift: Schweizer Münzblätter = Gazette numismatique suisse = Gazzetta numismatica svizzera

Herausgeber: Schweizerische Numismatische Gesellschaft

Band: 70 (2020)

Heft: 278

Artikel: Chemical and isotopic characterization and production technique of subferrate asses of the Lyons Altar series

Autor: Klein, Sabine / Kaenel, Hans-Markus von

DOI: https://doi.org/10.5169/seals-881028

Nutzungsbedingungen

Die ETH-Bibliothek ist die Anbieterin der digitalisierten Zeitschriften auf E-Periodica. Sie besitzt keine Urheberrechte an den Zeitschriften und ist nicht verantwortlich für deren Inhalte. Die Rechte liegen in der Regel bei den Herausgebern beziehungsweise den externen Rechteinhabern. Das Veröffentlichen von Bildern in Print- und Online-Publikationen sowie auf Social Media-Kanälen oder Webseiten ist nur mit vorheriger Genehmigung der Rechteinhaber erlaubt. Mehr erfahren

Conditions d'utilisation

L'ETH Library est le fournisseur des revues numérisées. Elle ne détient aucun droit d'auteur sur les revues et n'est pas responsable de leur contenu. En règle générale, les droits sont détenus par les éditeurs ou les détenteurs de droits externes. La reproduction d'images dans des publications imprimées ou en ligne ainsi que sur des canaux de médias sociaux ou des sites web n'est autorisée qu'avec l'accord préalable des détenteurs des droits. En savoir plus

Terms of use

The ETH Library is the provider of the digitised journals. It does not own any copyrights to the journals and is not responsible for their content. The rights usually lie with the publishers or the external rights holders. Publishing images in print and online publications, as well as on social media channels or websites, is only permitted with the prior consent of the rights holders. Find out more

Download PDF: 20.12.2025

ETH-Bibliothek Zürich, E-Periodica, https://www.e-periodica.ch

Chemical and isotopic characterization and production technique of subferrate *asses* of the Lyons Altar series

Sabine Klein,
Hans-Markus
von Kaenel

The early Roman Imperial *AES* Coinage IV.

Content

Part I (already published in March 2020 in SM 70, fascicle 277, pp. 3–21)

Part II

S. Klein, H.-M. von Kaenel: Chemical and isotopic characterization and production technique of subferrate *asses* of the Lyons Altar series, SM 70, 2020, S. 43–56.

4. Analytical data and their discussion

4.1. Chemical analysis

As a first screening and before cutting coin 4, it was analyzed semi-quantitatively with a tabletop energy dispersive micro X-ray fluorescence spectrometer (ED-µ-XRF). This analytical setup only records the surface of the coins, so that mainly the copper layer was analyzed and not the inner material, the iron flan. The surface analysis shows copper metal with 6–13 % iron and about 0.5 % zinc and lead *(Table 1)*.

Element:	Wt% (n = 4)	Method	
SnL	0.18	kV	40
V K	0.04	uA	50
CrK	0.02	Itera.	4
MnK	0.18	Live Tm	100
FeK	9.45	Reso	137.2
CoK	0.09	Method	FP-NoStds
NiK	0.18		
CuK	89.00		
Znk	0.55		
AsK	0.06		
PbL	0.25		
Total	100.00		

Table 1: Energy dispersive µ-XRF on the cut and polished surface of the subferrate coin 4. The method is non-invasive and the semi-quantitative analysis represents the surface of the coin (copper layer). The iron is microstructurally present as inclusions, so that individual spot analyses differ slightly from each other. The present table is a case example for copper metal used for coating. Quantification: Standardless fundamental parameter calculation (Wt% = weight percentage; n = 4; 4 sample spots analysed).

A quantifiable and more precise elemental analysis was performed with wavelength dispersive electron beam microanalysis[67]. The iron flan is made of very pure iron (> 99 %), carbon is not detectable by the method. The total trace element content is < 1 %. The copper layer is also completely pure copper, with the exception of iron, which was identified microscopically as a dendritic component *(Table 2)* and has a bulk concentration of about 4 % in the copper metal. The copper metal (based on a recalculated analysis) also contains traces of additional elements. Provenance-leading elements may be increased amounts of antimony and silver, accompanied by lower levels of arsenic, tin, lead, sulphur and manganese.

67 Wavelength dispersive Jeol Superprobe EPMA 8900 RL, accessible at the electron microscopy laboratory at Goethe-University Frankfurt a. M.

EPMA 23.12.2018	n	Cu	Fe	Sb	As	Sn	Ni	Ag	Pb	Co	S	Mn	Zn	Cd	Total	Total (as analysed)
Iron core	20	0.023	99.684	0.007	0.036	<DL	0.028	0.007	<DL	0.165	0.021	0.019	0.021	0.014	100	101.814
Copper skin	20	95.208	4.273	0.096	0.034	0.034	0.164	0.112	0.019	0.004	0.025	0.015	0.000	0.016	100	100.306
Fe in copper skin	9	12.865	86.370	0.009	0.024	0.003	0.540	0.010	0.001	0.146	0.008	0.014	0.002	0.009	100	100.944
Recalculated: copper skin		99.458		0.100	0.036	0.036		0.117	0.020		0.026	0.015	0.000	0.017	100	
Recalculated: iron inclusions			99.121				0.619			0.168		0.016	0.002		100	

Table 2: WD-EPMA of the subferrate coin 4. Analysis of the iron flan and the copper layer. Point analysis was done with electron beam size of 6 µm, 20 kV and 30 nA. Element concentration in weight%; results as averaged from number of analysis. Values normalized to 100 % total, original totals of single point analysis are presented in last column. Carbon content is not detectable by EPMA. The analysis of iron inclusions (see table: "copper skin"; "Fe in copper skin") catches also the copper matrix, because the iron inclusions are sometimes smaller than the electron beam diameter, so that a mixed analysis of the iron inclusions with copper metal result. The same is for the copper matrix, in which some iron cannot be excluded, if the electron beam defines the area of analysis. Therefore, recalculated analyses are presented in the last two lines of the table, which better reflects the true composition of the copper matrix resp. the iron inclusions.

As far as the α-iron dendrites in the copper layer are concerned, the WD-EPMA analysis (recalculated) shows clearly elevated nickel: 0.6 % Ni and cobalt: 0.7 % Co content compared to the iron flan itself *(Fig. 13)*. The iron used for the composite materials, consisting of iron flan and copper plating, is therefore different in composition.

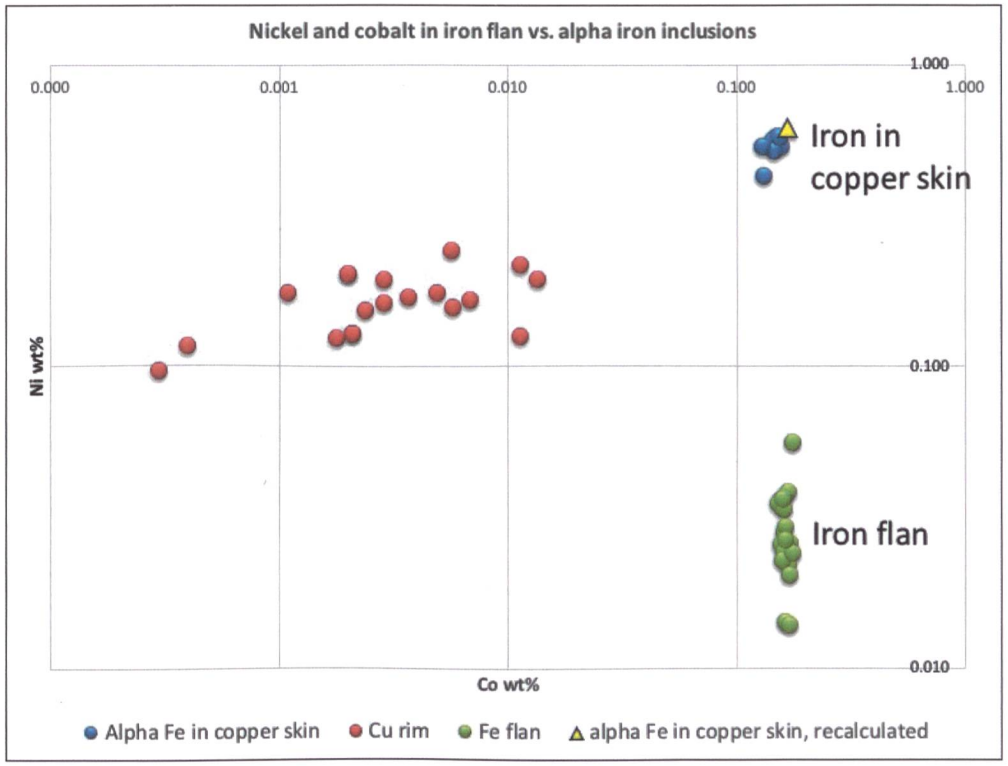

Figure 13: Differences in nickel concentration in iron flan and plating according to the WD-EPMA analyses.

This was also confirmed by a laser ablation ICP-MS analysis[68] *(Fig. 14)*. The differences lie in particular in the elements nickel, chromium, cobalt, zinc and selenium, which are increased in the iron inclusions in copper. Manganese, on the other hand, is much lower in the iron inclusions than in the iron flan.

68 Frankfurt Isotope and Element Center (FIERCE) at Goethe-University Frankfurt a. M.

S. Klein, H.-M. von Kaenel: Chemical and isotopic characterization and production technique of subferrate *asses* of the Lyons Altar series, SM 70, 2020, S. 43–56.

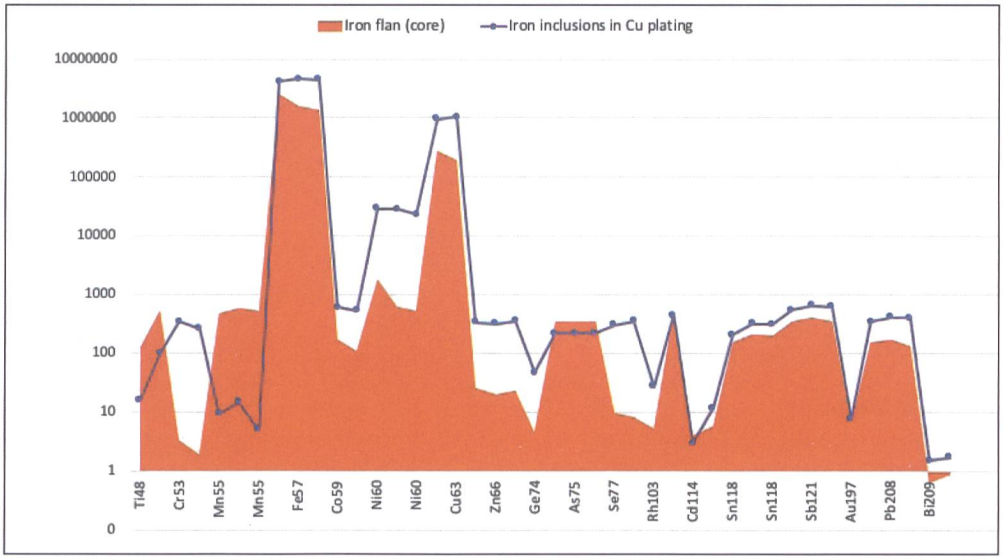

Figure 14: Laser ICP-MS analysis of the subferrate coin 4 for the comparison of iron in the copper plating and iron of the flan. The differences are clearly visible in elements such as nickel, cobalt and others. Isotopes of the elements were measured simultaneously and calculated against three internal standards, which contain different trace element composition – not all elements are contained in all three standards. Visualized is a collection of elements useful for the demonstration of differences and similarities. Some elements are listed double, because they were calculated individually on the base of two standards, but are in good consistence to each other, as was expected from the high-precision method. The number behind the element symbol is indicative for the particular isotope.

4.2. Lead isotope analysis and provenance of the copper metal used for the plating

Samples were taken by drilling 1 mm diameter steel (HSS) drills into the edges of coins 1 and 4. The sampling procedure was as follows: a–c represents a profile from the outer surface to the deeper area, where "a" reflects the outer surface of the plating (in case of coin 1 completely corroded metal), "b" is the uncorroded copper plating and "c" reached the iron flan. Because the copper layer is so thin, "b" is mixed material of copper and iron metal.

Samples were dissolved and column separated to isolate lead from copper using a laboratory standard protocol, thus gaining a concentrated lead solution. The sample solution enriched in lead was then dissolved in 1 ml double distilled 2 % HNO_3 to which 100 ppb of a thallium standard solution (NIST SRM 997, $^{205}Tl/^{203}Tl$) was added to correct internal mass fractionation. Lead isotope analysis was performed with a multi-collector ICP mass spectrometer (Neptune, ThermoFinigan, Goethe University Frankfurt, Faculty of Geosciences/Geography, now FIERCE Laboratory). The four isotopes ^{204}Pb, ^{206}Pb, ^{207}Pb and ^{208}Pb were analyzed. A common standard reference material for lead (NIST SRM 981) was measured as unknown samples after every 10 samples to monitor the drift of the instrument, which affects the quality of the measurements. Acid blanks were measured as first and last samples. The isotope ratios $^{206}Pb/^{204}Pb$; $^{207}Pb/^{204}Pb$; $^{208}Pb/^{204}Pb$; $^{207}Pb/^{206}Pb$; $^{208}Pb/^{206}Pb$ are used in geochemistry and archaeometallurgy for data interpretation, analytical errors were calculated from the individual measurements.

The analysis of the two subferrate coins, three samples each, shows that the upper surface of the coins represented by the samples "a" has a different lead isotope ratio than the samples "b" and "c" *(Table 3)*. Although the metal is different for "b" and "c", their lead isotope signatures are very close to each other. "b" and "c" are certainly the more valuable results for the coins, as the upper side ("a") might be changed by alteration processes and therefore does not represent the true composition. Although of different metal, "b" as representing the copper layer (mixed with some material from the underlying flan) is in good comparison with "c", which is the iron layer. It is difficult to explain from two samples why copper and iron metal are so close to each other in lead isotope signature. It is predictable, that copper for the plating and iron might not necessarily come from the same geological environment and thus from the same region, but this is indicated for the two investigated coins in this case study. Further studies on more subferrate coins would help, if more coins could be sampled micro-invasively.

Coin		$^{206}Pb/^{204}Pb$	2sigma	$^{207}Pb/^{204}Pb$	2sigma	$^{208}Pb/^{204}Pb$	2sigma	$^{207}Pb/^{206}Pb$	2sigma	$^{208}Pb/^{206}Pb$	2sigma
1a	Augustus, Lyons Altar series I	18.66622	0.01840	15.65678	0.01619	38.57526	0.04239	0.83877	0.00022	2.06669	0.00052
1b		18.43851	0.01103	15.62638	0.00964	38.39851	0.02583	0.84748	0.00015	2.08249	0.00042
1c		18.43931	0.06284	15.61830	0.05436	38.39902	0.13421	0.84700	0.00057	2.08225	0.00110
4a	Augustus, Lyons Altar series I/II	18.69394	0.01356	15.67048	0.01160	38.71168	0.02869	0.83826	0.00017	2.07079	0.00036
4b		18.42585	0.00828	15.63282	0.00693	38.41292	0.02065	0.84841	0.00011	2.08476	0.00038
4c		18.42604	0.02916	15.63173	0.02549	38.41355	0.06235	0.84835	0.00022	2.08468	0.00050

Table 3: Lead isotope ratios measured with MC ICP-MS. Coins 1 and 4. The three micro-samples each are taken as a profile. a = surface material, b = copper plating, c = iron flan.

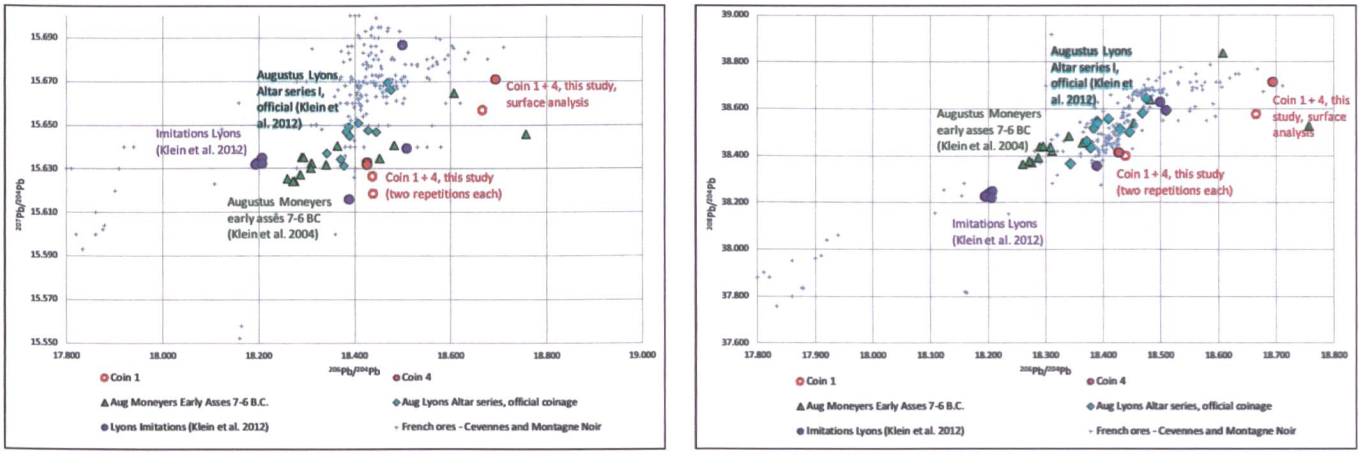

Figure 15 a.b: Lead isotope diagrams of coins 1 and 4 sampled by drilling and measured by MC ICP-MS (3 measurements each, red filled and open circles) at FIERCE Laboratory, Goethe-University Frankfurt. Left: horizontal axis = $^{206}Pb/^{204}Pb$, vertical axis = $^{207}Pb/^{204}Pb$, right: horizontal axis = $^{206}Pb/^{204}Pb$, vertical axis = $^{208}Pb/^{204}Pb$. The two sample points in the upper right corner of the diagram (1 filled red, 1 open red circle) are sample "a" from the surface of the coins (copper with corrosion) and have higher ratios. "b" and "c" material plots in some distance in the more center diagram and are from the copper layer and the iron flan. For comparison, Early Augustan *asses* (Klein et al. 2004) are plotted as green triangles, official Augustus Lyon Altar series I coins as blue diamonds and the imitations as purple circles (Klein et al. 2012).

S. Klein, H.-M. von Kaenel: Chemical and isotopic characterization and production technique of subferrate *asses* of the Lyons Altar series, SM 70, 2020, S. 43–56.

Comparison of the lead isotope signature of the copper metal *(Fig. 15a.b)* used for the subferrate coins with contemporary Augustan moneyer *asses*[69], official LAS I/II series coinage from Lyons and Lyons imitations[70] gives no perfect match, but some relation is indicated by the lead isotopes. Closest is the official LAS I/II series coinage investigated earlier, whereas the Lyons imitations are in farest distance of all. It could be quickly concluded from the impure copper used, which is characterized by iron content, that recycled material or comparably impure copper was used for the copper plating of coin 4.

Searching for a match with potential ore deposits, and in coincidence with our earlier observations on the official Lyon altar series copper coinage, the use of French ores as a metal source for the two subferrate coins are very plausible. However, it must be considered that the analysis carried out here have only case study character rather than statistical relevance.

5. Production technique of coin 4

5.1. Different techniques for the production of plated coins

The metallographic examination is helpful for the identification of the different techniques. Several criteria help to decide between the proposed techniques or to exclude them: Observations on material exchange from iron flan to copper skin, microstructural evidence on casting versus cold or hot forming or chemical measurements at the interface between iron flan and copper skin.

The description of the metallographic phenomena of the coin was presented in chapters 2.2. and 2.3. The technique used by M. Pfisterer and R. Traum represents a reliable reference for the microstructures resulting from hot copper plating, the *Feuerverkupferung* and is described below before a comparison and conclusion is drawn on the applied technique to produce coin 4.

Intensive studies exist about plating techniques for copper-core silver plated (subaerate) Greek and Roman copper cores[71], other techniques and variants are described multiply in literature[72]. In the following, a brief summary is presented:
Eutectic soldering (for plating copper with silver): Attaching a silver foil to a copper core by means of silver solder uses the physical property of the eutectic alloy composition of silver and copper to achieve the lowest melting temperature of any mixture of the two. Campbell presented a 1933 drawing visualizing the intermetallic layer of eutectic silver-copper (solder) over the copper core. The ends of the thin foil overlap at the edges of the coin[73]. This coating technique should not work with copper and iron, because the binary system does not allow eutectic composition.

Self-soldering (described for coating copper with silver): In other examples, the silver was bonded to the copper by heating to eutectic temperature without the use of a solder alloy. The bond is achieved by diffusion. The eutectic temperatures[74] allow only a limited melting of the composite materials[75].

Immersion in molten copper (described for coating copper with silver): It is possible to produce silver plating by immersing the copper flan in a bath of

69 Klein et al. 2004, p. 474 Tab. 1.
70 Klein et al. 2012, pp. 105–107 Tab. 2.
71 Cope 1972; Campbell 1933.
72 For terminology see Scott 1991, App. E; for copper plating on iron see Corefield 1993.
73 Campbell 1933, Fig. 72 (coin 9, drawing) and Fig. 97 (coin 13, drawing).
74 Eutectic temperatures: Cu-Ag = 779 °C; Fe-Cu = no eutectic system.
75 La Niece 1993, p. 228.

molten (potentially eutectic) silver-copper alloy, then removing the wetted coins from the melt and solidifying the plating material[76]. This results in a very thin silver layer. If the dipping is not repeated several times, only a very thin copper skin will result, which is very heterogeneous in thickness. The resulting microstructure of the plated metal would be that of a casting process, resulting in dendritic grains.

S. Klein, H.-M. von Kaenel: Chemical and isotopic characterization and production technique of subferrate *asses* of the Lyons Altar series, SM 70, 2020, S. 43–56.

Feuerverkupferung – hot plating with metal chips or powder: This technique works with various flan and plating metals, i.e. also when plating an iron flan with copper. A paste of copper chips or powder, borax powder and distilled water[77] is applied to the flan base until the silver has melted. An alternative process is described using the manteling with clay[78]. During the production and shaping of the flans, metal scale adheres to the surface of the cake, which must be carefully removed. In the literature[79] it is referred to as the diffusion reaction technique, a process which results in a plated layer which is applied to the iron or steel flange at approx. 1000 °C. The process influences the dissolution of the two metals in direct contact. This technique produces an irregular coating, and if the scale is not completely removed, it can be seen as sharp-edged inclusions in the plated layer. Microstructurally, copper is impregnated into the intergranulars or veins of the iron flan[80, 81], as a result of *"liquid metal embrittlement"*.

Sintering (described for the coating of copper on iron): A powder mixture of copper and iron as in modern powder metallurgy is heated sharply below the melting point, which forces diffusion, but prevents the powdered particles from total melting. The "liquid-phase sintering" of metal powders causes local oxidation in the grain interstices[82] and is therefore easy to identify metallographically.

Lost wax process: This coating technique starts with a metal flan as a core. Then two wax layers of the same thickness as the desired plating layer were modelled and pressed firmly onto the ob- and reverse of an official coin[83, 84]. The wax casting process was then continued in the common way, using a mold to embed flan and wax model. With the pouring of molten plating metal, the wax burns and evaporates, leaving space for the casting metal. In this way, the metal flan can be plated and is immediately a finished coin without the need for further striking. The microstructure of such coatings result as undistorted dendritic structures.

Refinement by wrapping: A process called *Überschmieden*[85] – overforging – uses a copper sheet, presumably by heating the iron flan to the melting temperature of copper (1085.5 °C), then wrapping the iron flan with a copper foil and hammering to bond the two materials together. The result is a metallographically visible structure of copper, which is cold or hot formed and leaves compressed and elongated copper grains in the copper layer. The iron flan is potentially not mechanically influenced by this process. It should be stressed that the microstructure of the plating layer could be affected later by the striking of the coin, making it difficult to distinguish the two processes, all the more so if the two processes were applied later.

76 Tylecote 1979.
77 Pfisterer – Traum 2005a and b.
78 Ankner – Hummel 1985.
79 Zwicker – Dembski 1988, p. 61.
80 Pintz 2014, Figs. 2.4 and 2.5.
81 Haubner et al. 2016, p. 450.
82 Velasques Ugarteche et al. 2015.
83 Gruel et al. 2011.
84 Greul – Popovitch 2007, pp. 28–31.
85 Tylecote 1986.

S. Klein, H.-M. von Kaenel: Chemical and isotopic characterization and production technique of subferrate *asses* of the Lyons Altar series, SM 70, 2020, S. 43–56.

5.2. Experimentally produced copper plating on iron flans by M. Pfisterer and R. Traum

M. Pfisterer and R. Traum of the Kunsthistorisches Museum in Vienna carried out experiments using Roman *Falschmünzer* technology. They experienced the necessary production steps to obtain a complete example of a subferrate coin with *Feuerverkupferung*. R. Traum was so generous as to leave us one of his experimental products for metallographic comparison with coin 4.

For the experiments, cylindrical ferrous metal slices were hammered to the desired thickness under repeated annealing conditions and the rims became barrel-shaped *(Fig. 16)*. The porosity is perpendicular to the direction of stress. Pfisterer & Traum's hot copper plating results in a thin copper layer not extending 200 µm in thickness. Only very few iron inclusions in copper can be identified by SEM in an angular shape *(Fig. 17)*. These are clearly remains of iron scale which are formed during annealing and hammering to flatten the iron flan. The EDS analysis records a total sum of 6–8 % by weight of Fe in the copper layer.

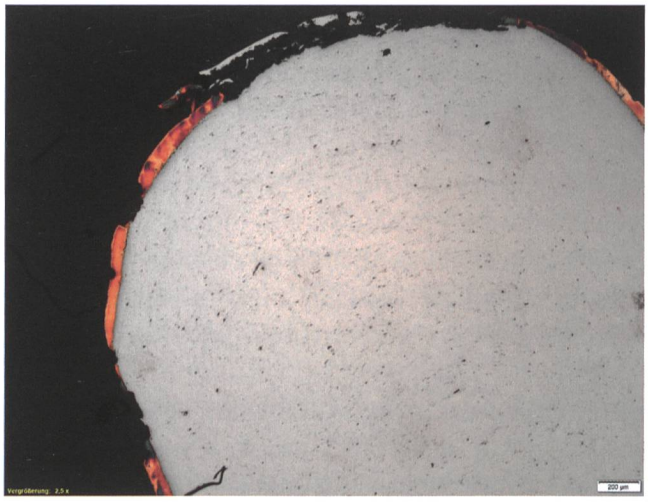

Figure 16: Barrel shape of iron flan from the experiment.
The copper layer is compared to coin 4 thin and irregular in thickness.

Figure 17: Experiment under SEM (backscattered electron image).
Above: Copper coating with iron tinder inclusions (black), below iron flan with black aligned pores.

At the interface between copper and iron and along grain boundaries the copper migrated and disseminated in the molten state into the solid ferrous metal *(Fig. 18)* as volume diffusion at high or low temperatures or as grain boundary diffusion at low temperatures[86]. Porosity in copper is concentrated along the interface between copper and iron flan *(Fig. 19)*.

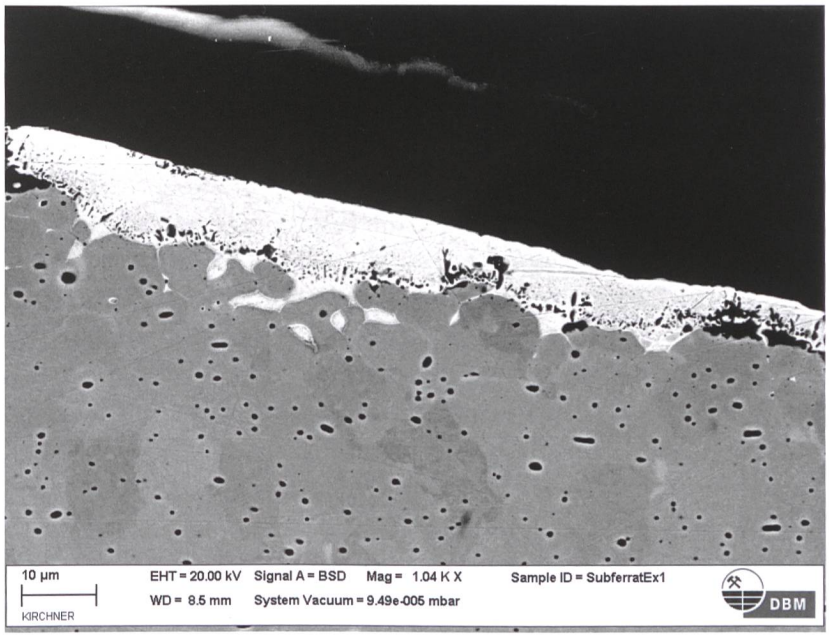

Figure 18: Backscattered electron image of the experiment. Reaction zone between iron flan and copper skin. The interface is not as sharp as in the subferrate coin. There is exchange between iron and copper layer, the copper intruding into the intergranulars of the iron metal. In the copper layer, porosity is concentrated horizontally close to the iron interface. The iron flan has closed porosity (black) estimated as around 10–15 % and is heterogeneous in composition, which is visible in the backscattered image as different gray levels. Within the iron metal and close to the copper layer, the grain boundaries appear brighter, which indicates intergranular enrichment of copper in the iron.

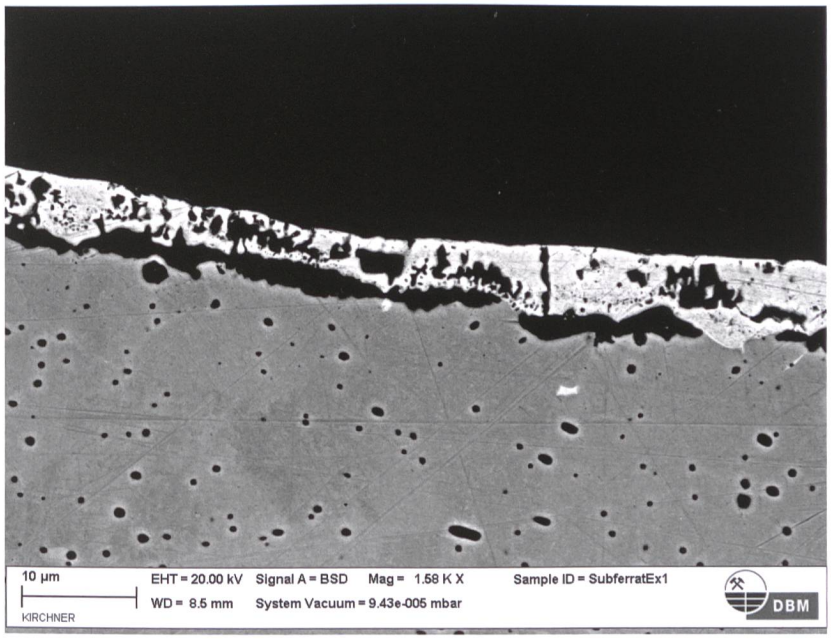

Figure 19: Backscattered electron image of the experiment. Porosity weakens the adherence between the copper layer and the iron flan.

S. Klein, H.-M. von Kaenel: Chemical and isotopic characterization and production technique of subferrate *asses* of the Lyons Altar series, SM 70, 2020, S. 43–56.

86 Ishida 1986, pp. 1171–1172.

S. Klein, H.-M. von Kaenel: Chemical and isotopic characterization and production technique of subferrate *asses* of the Lyons Altar series, SM 70, 2020, S. 43–56.

5.3. Arguments for the application technique of sheet copper for coin 4

Based on the evidence on coin 4 and the comparison with the microstructural phenomena in R. Traum's experimental product, the use of a copper sheet with a constant thickness of 300–350 µm wrapped around the hammered iron flan is preferred. The sheet had sharp and cut edges. The ends of the sheets were joined by a special treatment under overfired conditions. Coin 4 appears microstructurally different along the edges compared to the planes of the flan. The copper layer tightly seals the iron flan and thus protects it from corrosion, with the exception of the barrel-shaped edges where the copper layer is broken up. The adhesion of the copper layer to the iron is distorted here. Sharp cuts are present. An overheated ferrite-pearlite microstructure has been identified for the iron flan, which indicates that the spatial joining process involves heat treatment.

The etching of coin 4 shows the copper layer with almost undistorted α-iron dendrites[87]. This structure proves that it was originally a copper casting and was subsequently densified by cold working, indicated by the absence of annealing structures. The harder iron in copper is less influenced by the working process, so that the dendritic shape is still clearly visible.

In contrast to the experiment in which the copper plating was produced by a copper-borax melt, which produces a thin layer of irregular thickness, the copper layer of coin 4 is significantly thicker and of constant thickness. The interface between iron flan and copper layer is extremely defined (sharp) and without interfacial reactions as they occur in *Feuerverkupferung,* soldering or sintering. The question arises how the iron was introduced into the copper metal of the layer. There are several considerations: (a) It was previously assumed that it was practically possible to reach temperatures up to the melting point of the iron (experiments by J. Merkel[88]), which could lead to the migration of (partially) molten iron from the flan into the copper layer. However, this is not important here, as the microstructure gives no indication that molten iron has penetrated the interface into the copper layer. (b) This is reinforced by the fact that the iron flan is very pure of trace elements and has been defined as low carbon steel by microstructural analysis. Instead, the composition of the ferrous metal used for the flan differs greatly from that of the iron dendrites in the copper metal. This was proven by the results of the elemental analysis. (c) The iron inclusions in the copper layer represent dendritic α-iron in the phase matrix of ε-copper. This microstructure can form at about 1200 °C. In view of smelting experiments recently carried out by one of us with copper sulphide minerals[89], the temperatures in a copper smelting furnace may reach even higher temperatures. Molten copper can absorb metallic iron in the reduction zone of the furnace as copper passes through the slag and accumulates at the bottom of the furnace. Second, iron could diffuse into copper metal if reduced from a slag that forms a copper-iron alloy between solidus and liquidus temperatures.

Metallic iron in copper metal was not observed in contemporary Roman Imperial copper coins so far[90]. In archaeometallurgical context, iron is usually reported as a major component in copper as related to the production of unrefined copper from smelting processes. Cooke & Aschenbrenner 1975 state that metallic iron

87 Scott 1991.
88 Pfisterer – Traum 2005a and b.
89 Rose et al. 2019, pp. 44–45.
90 Klein – von Kaenel 2000.

"is not representative of a finished product, but is instead material that has been discarded during refining or re-melting."

S. Klein, H.-M. von Kaenel: Chemical and isotopic characterization and production technique of subferrate *asses* of the Lyons Altar series, SM 70, 2020, S. 43–56.

5.4 Numismatic conclusions

The technical and temporal effort required to produce subferrate *asses* of the Lyons Altar types in the manner described here will have been considerably greater than to coin a copper blank. Did the weight of the copper skin of 3.4 g calculated for coin 4 represent a "gain" for this coin, which in view of the special manufacturing process represented an incentive to produce corresponding coins? If one takes the target weight of about 11.3 g for a regular Lyons Altar *as* of series I and of about 10.4 g for one of series II[91], it becomes evident that 3–4 copper foils for subferrate asses could have been produced from the copper of a regular coin. However, the iron core, which made up about 7–8 g iron, as well as the technical know-how and the effort would have to be taken into account in order to arrive at a realistic assessment. To "save" copper, however, it would have been much easier to produce underweight imitations in copper, which also happened much more frequently. In fact, already under Augustus we find local imitations[92] of Augustan coin types in copper and brass, which can be recognized by their poor workmanship, their low weight and the "awkward" style. The imitations of Lyons Altar *asses* that we have studied[93] earlier oscillate between 3.8 and 10.2 g with a focal weight of 5–6 g, and were thus well distinguishable from the regular ones. A skillfully made subferrate *as,* on the other hand, hardly differed from a regular coin by its weight and its copper skin, provided that it was intact. In case of suspicion, however, it would have been easy possible for any fine blacksmith to assay a corresponding specimen.

The determined thickness of the copper skin of coin 4 (0.3–0.4 mm) is in accordance with the silver skins of subaerate *denarii* and *quinarii.* The thickness of the silver skins of eight metallurgically assayed subaerate *denarii*[94] is 0.1–0.5 mm. In the Oppidum of Rheinau-Altenburg, six corroded silver skins[95] to produce subaerate *quinarii* were found. Due to the thickness of the copper core around which the silver foils had to be wrapped, their diameter is slightly larger than the diameter of the core and their weight is about 0.3 g, i.e. approx. 0.6 g per *quinarius* with a target weight of 1.5–1.7 g. This means that a "saving" of silver per *quinarius* would have existed in almost one third of its target weight.

While the argument that in certain regions of the Latène culture and at certain times it was quite difficult to obtain silver for local minting may be true, and Gresham's law that good silver displaced bad silver did – perhaps – not fail to have some effect, one would be surprised if the same arguments had applied equally to the coin metal copper in the Julio-Claudian period. According to the lead isotope ratios, the copper of the two subferrate Lyons Altar *asses* 1 and 4 analysed here does not seem to have been obtained by melting down corresponding regular coins, but was of a different origin. Whether from this fact alone an indication of a production of these coins as "counterfeits" can be derived seems doubtful, rather they fit into the context of the tolerance of unofficial local minting in the given area in the early imperial period outlined above. What was also

91 Giard 1983, p. 46
92 See note 23.
93 Klein et al. 2012, pp. 100–102.
94 Anheuser 1998, pp. 135–136; Anheuser – Northover 1994, pp. 23–25.
95 Nick 2019, pp. 165–168, specially 166 with Fig.173e; Nick 2015, p. 1616.

possible is documented by the already mentioned[96] deposit of about 100 coins from the Haltern necropolis, whose core consists of lead and which show small traces of a copper skin. As emphasized above, knowing more about the local practices handling of the imitations and subferrate coins would illuminate our knowledge of the functions of small coinage in the first decades of the first century AD.

To conclude with a practical suggestion: In order to detect the iron cores in plated coins, numismatists working with coin finds should systematically examine coins with a magnet.

Acknowledgements

Our thanks go at first to the finders of the coins, Jörg Lotter and Michael Paulsen, and to Thomas Becker from the Abteilung hessenARCHÄOLOGIE des Landesamtes für Denkmalpflege Hessen, Aussenstelle Darmstadt, who supported us just as Markus Helfert, Karlheinz Engemann, Thomas Maurer and Markus Scholz. For numismatic advice we are grateful to Frank Berger, Nathan T. Elkins, Michael Nick and Markus Peter. Peter Northover made helpful comments concerning our metallographic interpretation. We would like to thank René Traum, Kunsthistorisches Museum Wien, for providing one of his flans, an experimental product, for investigating the joining techniques of subferrate coins. FIERCE is financially supported by the Wilhelm and Else Heraeus Foundation and by the Deutsche Forschungsgemeinschaft (DFG, INST 161/921-1 FUGG and INST 161/923-1 FUGG), which is gratefully acknowledged. This is FIERCE contribution No. 12. Andreas Ludwig (DBM) has helped with the preparation of the polished specimen and Dirk Kirchner (DBM) operated the REM. We are grateful for Samuel Nussbaum's and Ruedi Kunzmann's editorial support.

Photographic credits: Coins 1, 4 were made with a photographic instrument of the Römisch-Germanische Kommission (RGK), Frankfurt a. M. We thank J. Lotter for the photograph of coin 2, and M. Paulsen for coin 3.

Translation and language improvement were partly undertaken with www.DeepL.com/Translator (free version).

Sabine Klein (Metallurgie, Analytik, Technik)
Forschungsbereich Archäometallurgie
Deutsches Bergbau-Museum Bochum
Am Bergbaumuseum 31
44791 Bochum, Germany
sabine.klein@bergbaumuseum.de

and also

96 Ilisch 1999, pp. 285–286; see also note 41.

Frankfurt Isotope and Element Research Center (FIERCE)
Goethe-Universität Frankfurt am Main
60438 Frankfurt am Main, Germany

Hans-Markus von Kaenel (Archäologie, Numismatik)
Goethe-Universität Frankfurt am Main
Institut für Archäologische Wissenschaften, Abt. II
Norbert-Wollheim-Platz 1
60629 Frankfurt am Main, Germany
v.kaenel@em.uni-frankfurt.de

S. Klein, H.-M. von Kaenel: Chemical and isotopic characterization and production technique of subferrate *asses* of the Lyons Altar series, SM 70, 2020, S. 43–56.

References Part II

Anheuser 1998
K. Anheuser, Silver-Plated-on-Iron Roman Coins, in: W.A. Oddy – M.R. Cowell (eds.), Metallurgy in Numismatics 4, Royal Numismatic Society Special Publication 30 (London 1998), pp. 134–146.

Anheuser – Northover 1994
K. Anheuser – P. Northover, Silver Plating on Roman and Celtic Coins from Britain - A Technical Study, The British Numismatic Journal 64, 1994, pp. 22–32.

Ankner – Hummel 1985
D. Ankner – F. Hummel, Kupferlote und Verkupferung auf Eisen, Arbeitsblätter für Restauratoren, Vol. 18/2, 1985, pp. 196–206 (AATA 23-1178).

Campbell 1933
W. Campbell, Greek and Roman plated coins, ANSNNM 57 (New York 1933).

Cope 1972
L.H. Cope, Surface-silvered ancient coins, in: E.T. Hall – D.M. Metcalf (eds.), Methods of chemical and metallurgical investigation of ancient coinage, Royal Numismatic Society, Special Publication 8 (London 1972), pp. 261–278.

Corefield 1993
M. Corefield, Copper plating on iron, in: S. La Niece – P. Craddock (eds.), Metal Plating and Patination – Cultural, Technical and Historical Developments (Oxford 1993), pp. 276–283.

Giard 1983
J.-B. Giard, Le monnayage de l'atelier der Lyon des origines au règne de Caligula (43 avant J.-C. – 41 après J.-C.), Numismatique Romaine 14 (Wetteren 1983).

Gruel et al. 2011
K. Gruel – D. Lacoste – C. Fraresso – M. Pernot – F. Allier, Données expérimentales sur la fabrication de quinaires gaulois fourrés, in: N. Holmes (ed.), Proceedings of the XIV^th International Numismatic Congress Glasgow 2009, Vol. 2 (Glasgow 2011), pp. 1173–1181.

Gruel – Popovitch 2007
K. Gruel – L. Popovitch (eds.), Les monnaies gauloises et romaines de l'oppidum de Bibracte, Collection Bibracte 13 (Glux-en-Glenne 2007).

Haubner et al. 2016
R. Haubner – S. Strobl – J. Zbiral – C. Gusenbauer – U. Pintz, Metallurgical Characterization of a coated Roman Iron Coin by Analytical Investigations, Archaeometry 58, 3, 2016, pp. 441–452 (DOI: 10.1111/arcm.12179).

Ilisch 1999
P. Ilisch, Die Münzen aus den römischen Militäranlagen in Westfalen, in: W. Schlüter – R. Wiegels (eds.), Rom, Germanien und die Ausgrabungen von Kalkriese. Internationaler Kongress der Universität Osnabrück und des Landschaftsverbandes Osnabrücker Land e. V. vom 2.–5. September 1996, Osnabrücker Forschungen zu Altertum und Antike-Rezeption 1 (Osnabrück 1999), pp. 279–291.

S. Klein, H.-M. von Kaenel: Chemical and isotopic characterization and production technique of subferrate *asses* of the Lyons Altar series, SM 70, 2020, S. 43–56.

Ishida 1986
T. Ishida, The interaction of molten copper with solid iron, Journal of Material Science 21, 1986, pp. 1171–1179.

Klein – von Kaenel 2000
S. Klein – H.-M. von Kaenel, The early Roman Imperial *AES* Coinage I: Metal Analysis and Numismatic Studies: The Chemical Profile of Copper Coins of the Rome Mint from Augustus to Claudius, SNR 79, 2000, pp. 53–106.

Klein et al. 2004
S. Klein – Y. Lahaye – G.P. Brey – H.-M. von Kaenel, The early Roman Imperial *AES* Coinage II: Tracing the copper sources by analysis of lead and copper isotopes – copper coins of Augustus and Tiberius, Archaeometry 46, 3, 2004, pp. 469–480 (DOI: 10.1111/j.1475-4754.2004.00168.x).

Klein et al. 2012
S. Klein – H.-M. von Kaenel – Y. Lahaye – G.P. Brey, The early Roman Imperial *AES* Coinage III: Chemical and isotopic characterization of Augustan copper coins from the mint of Lyons/Lugdunum, SNR 91, 2012, pp. 63–110.

Nick 2019
M. Nick, Die spätlatènezeitlichen Münzen aus Rheinau, in: P. Nagy, Archäologie in Rheinau und Altenburg. Prospektionen im schweizerisch-deutschen Grenzgebiet, Monographien der Kantonsarchäologie Zürich 51 (Egg 2019), pp. 165–168. 268.

Nick 2015
M. Nick, Die keltischen Münzen der Schweiz: Katalog und Auswertung I-III, IFS 12 (Bern 2015).

La Niece 1993
S. La Niece, Technology of Silver-Plated Coin Forgeries, in: M.M. Archibald – M.R. Cowell (eds.), Metallurgy in Numismatics 3, Royal Numismatic Society Special Publication 24 (London 1993), pp. 227–236.

Pfisterer – Traum 2005a
M. Pfisterer – R. Traum, Die Herstellungstechnik subferrater Kopien römischer Buntmetallmünzen: ein praktisches Experiment, SNR 84, 2005, pp. 125-140 (DOI: http://doi.org/10.5169/seals-175930).

Pfisterer – Traum 2005b
M. Pfisterer – R. Traum, Ein Experiment zur römischen Falschmünzertechnik, Technologische Studien 2, 2005, pp. 72–85.

Pintz 2014
U. Pintz, FMRÖ Salzburg – Die Fundmünzen der Villa Loig und ihre Besonderheit, die Eisenmünzen, Dissertation Universität Wien 2014.

Rose et al. 2019
T. Rose – E. Hanning – S. Klein, Experimente zur prähistorischen Kupferverhüttung im Labor für Experimentelle Archäologie, Archäologie Schweiz 2019/1, pp. 44–45.

Scott 1991
D. Scott, Metallography and Microstructure of Ancient and Historic Metals (The J. Paul Getty Trust 1991).

Tylecote 1979
R.F. Tylecote, A History of Metallurgy (London 1979).

Tylecote 1986
R.F. Tylecote, The Prehistory of Metallurgy in the British Isles (London 1986).

Velasques Ugarteche et al. 2015
C. Velasques Ugarteche – K. Pagnan Furlan – R. Do Vale Pereira – G. Trindade – R. Binder – C. Binder – A. Nelmo Klein, Effect of Microstructure on the Thermal Properties of Sintered Iron-copper Composites, Materials Research 18, 6, 2015, pp. 1176–1182 (DOI: http://dx.doi.org/10.1590/1516-1439.030915).

Zwicker – Dembski 1988
U. Zwicker – G. Dembski, Technisch-chemische Untersuchungen an subferraten Sesterzen, Mitteilungen der Österreichischen Numismatischen Gesellschaft 28, 1988, pp. 12–17.